Stem Cell Reports
Article

ISSCR

OPEN ACCESS

Insulin-like Growth Factor II: An Essential Adult Stem Cell Niche Constituent in Brain and Intestine

Amber N. Ziegler,[1,6] Qiang Feng,[5,6] Shravanthi Chidambaram,[1] Jaimie M. Testai,[1] Ekta Kumari,[1] Deborah E. Rothbard,[1] Miguel Constancia,[2,3,4] Ionel Sandovici,[2,4] Tara Cominski,[1] Kevin Pang,[1] Nan Gao,[5] Teresa L. Wood,[1,7] and Steven W. Levison[1,7,*]

[1]Department Pharmacology, Physiology and Neuroscience, New Jersey Medical School, Rutgers University, Newark, NJ 07103, USA
[2]University of Cambridge Metabolic Research Laboratories, MRC Metabolic Diseases Unit, Department of Obstetrics and Gynaecology, Cambridge CB2 0SW, UK
[3]National Institute for Health Research Cambridge Biomedical Research Centre, The University of Cambridge, Cambridge CB2 0SW, UK
[4]Centre for Trophoblast Research, The University of Cambridge, Cambridge CB2 0SW, UK
[5]Department of Biological Sciences, Rutgers University-Newark, Newark, NJ 07102, USA
[6]Co-first author
[7]Co-senior author
*Correspondence: levisosw@rutgers.edu
https://doi.org/10.1016/j.stemcr.2019.02.011

SUMMARY

Tissue-specific stem cells have unique properties and growth requirements, but a small set of juxtacrine and paracrine signals have been identified that are required across multiple niches. Whereas insulin-like growth factor II (IGF-II) is necessary for prenatal growth, its role in adult stem cell physiology is largely unknown. We show that loss of *Igf2* in adult mice resulted in a ~50% reduction in slowly dividing, label-retaining cells in the two regions of the brain that harbor neural stem cells. Concordantly, induced *Igf2* deletion increased newly generated neurons in the olfactory bulb accompanied by hyposmia, and caused impairments in learning and memory and increased anxiety. Induced *Igf2* deletion also resulted in rapid loss of stem and progenitor cells in the crypts of Lieberkühn, leading to body-weight loss and lethality and the inability to produce organoids *in vitro*. These data demonstrate that IGF-II is critical for multiple adult stem cell niches.

INTRODUCTION

Stem cells have long been of interest to developmental biologists; however, these cells have now gained the interest of the broader scientific community because of their potential to repair degenerating tissues. For example, neural stem cells (NSCs) and the new neurons that they produce are now recognized as necessary for learning and memory, for promoting cognitive function, and for their potential to replace neurons and glial cells lost as a consequence of brain injury or disease (Chojnacki et al., 2012; Lim and Alvarez-Buylla, 2014; Zhao et al., 2008). Similarly, adult intestinal stem cells (ISCs), which reside at the bottom of the crypt of Lieberkühn, constantly replenish the epithelial sheet for a lifespan, contributing to tissue homeostasis as well as mucosal regeneration after injury (Tetteh et al., 2014).

Stem cells naturally reside within specific niches where they receive local signals that maintain them in a primitive state. The niches for each adult stem cell population differ; thus, most of the factors that maintain tissue-specific stem cells exert local effects restricted to that niche. Only a limited number of juxtacrine or paracrine signaling factors have been identified that maintain stem cells residing in multiple niches; these include epidermal growth factor (EGF), Notch, Wnts, fibroblast growth factors (FGFs), Shh, and transforming growth factor β (Lander et al., 2012).

Insulin-like growth factor II (IGF-II) is highly expressed in the embryo and is necessary for normal embryonic and fetal growth (Baker et al., 1993; DeChiara et al., 1990; Liu et al., 1993; Ren et al., 2008; Shinar et al., 1993). In contrast, IGF-II is downregulated in most adult tissues, with notable exceptions including the brain and the intestine. In the adult CNS, IGF-II is produced by the choroid plexus, leptomeninges, endothelial cells, and stem/progenitor cells in the hippocampal subgranular zone (SGZ) (Bracko et al., 2012; Buono et al., 2015b; Ferron et al., 2015; Logan et al., 1994a, 1994b; Stylianopoulou et al., 1988). Due to production by the choroid plexus, IGF-II protein is found at high levels in the cerebral spinal fluid (Bunn et al., 2005). The sites of IGF-II expression place it in close proximity to the NSCs residing in the two major NSC niches: the subventricular zone (SVZ) of the lateral ventricle and the hippocampal SGZ. Moreover, although the *Igf2* gene is imprinted such that it is expressed only from the paternal allele in most tissues (DeChiara et al., 1991; Ferguson-Smith et al., 1991; Giannoukakis et al., 1993), it is biallelically expressed in choroid plexus, leptomeninges, and brain endothelial cells (Charalambous et al., 2004; DeChiara et al., 1991; Feil et al., 1994; Ferron et al., 2015).

Based on the expression data and our earlier studies on SVZ-derived neurospheres (Ziegler et al., 2012, 2014), we hypothesized that IGF-II might be an integral component

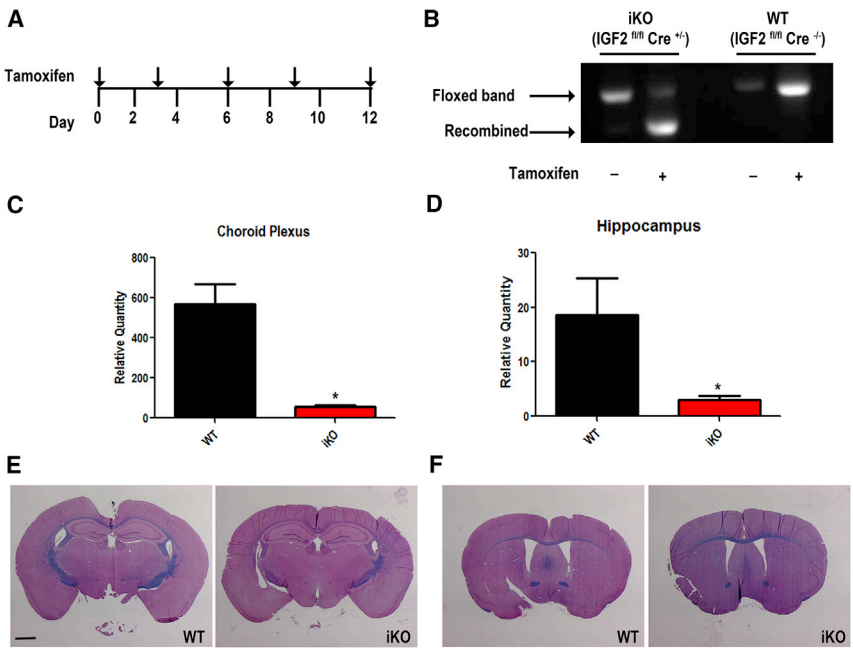

Figure 1. Tamoxifen-Induced Removal of *Igf2*

Schematic for tamoxifen dosing in C57BL/6 mice (A). PCR for the floxed *Igf2* allele at 449 bp in iKO mice ($Igf2^{fl/fl}$ $Cre^{+/-}$) with no tamoxifen or in WT mice ($Igf2^{fl/fl}$ $Cre^{-/-}$) or for the recombined allele at 384 bp in iKO mice ($Igf2^{fl/fl}$ $Cre^{+/-}$) plus tamoxifen (B). qPCR for *Igf2* mRNA in choroid plexus (C) and hippocampus (D) from samples collected 2 weeks post tamoxifen administration. See also Figure S1. Representative sections of Luxol fast blue and H&E stains at the level of the septal nuclei and the third ventricle of WT and iKO mice (E and F). Statistical significance: *$p < 0.05$ using ANOVA and Tukey's post hoc test, $n = 5$ WT and $n = 12$ iKO mice. Error bars represent SEM. Scale bar, 1 mm.

of the NSC niche. More recently, two studies provided support for IGF-II function in regulating NSCs; however, these studies did not address the function of IGF-II from multiple sources in regulating the adult NSCs. Bracko et al. (2012) demonstrated that *Igf2* mRNA is expressed by NSCs in the dentate gyrus (DG) but not by the NSCs in the SVZ. Thus, short hairpin RNA knockdown of *Igf2* mRNA reduced proliferation of DG NSCs but not SVZ NSCs. A second report by Ferron et al. (2015) demonstrated that deleting *Igf2* systemically beginning embryonically reduced the number of label-retaining cells in the SVZ and SGZ *in vivo*. However, loss of *Igf2* embryonically significantly reduces prenatal brain growth, making it impossible to separate the function of IGF-II in maintaining adult NSCs from a function in establishing NSCs during development. This study further demonstrated that loss of *Igf2* from endothelial cells beginning embryonically partially compromises SVZ NSCs but has no effect on the SGZ NSC population (Ferron et al., 2015), thus raising the question as to whether IGF-II is essential for maintaining the NSCs in the adult hippocampus.

In the intestine, IGF-II is found in the colonic mucosa, and *Igf2* loss of imprinting (LOI) in $Apc^{min/+}$ background increases crypt length (Sakatani et al., 2005). However, no studies to date have established whether IGF-II is an essential niche stem cell factor in the adult intestine. Therefore, to address the functions of IGF-II in multiple adult stem cell niches, we designed experiments to remove *Igf2* in young adult mice and evaluate adult NSC and ISC maintenance.

RESULTS

Adult NSCs Require Sustained IGF-II Production

To determine whether IGF-II is necessary for adult stem cell homeostasis, we mated floxed *Igf2* mice with a tamoxifen-inducible Rosa 26 CreER driver mouse line (Badea et al., 2003; Haley et al., 2012) to generate littermates for experimental animals that were all $Igf2^{fl/fl}$ and either Cre^{+} or Cre^{-}. Administering tamoxifen over 5 consecutive days beginning at postnatal day 21 (p21) resulted in death of *Igf2* knockout (KO) mice (see below regarding this lethal phenotype); therefore, we administered tamoxifen (75 mg/kg) every 3 days for the studies on the CNS (Figure 1A). PCR analysis 2 weeks after tamoxifen administration showed a recombined band of the expected size indicating excision of exons 4–6 of the *Igf2* gene (Figure 1B). Consistent with these results, mRNA levels of *Igf2* in choroid plexus and hippocampus were reduced by 90% in heterozygous Cre ($Igf2^{fl/fl}Cre^{+/-}$) mice versus wild-type (WT) ($Igf2^{fl/fl}$) (Figures 1C and 1D). Since *Igf2* mRNA levels were similarly reduced in mice heterozygous and homozygous for Cre (Figure S1), heterozygous Cre mice were used for all *in vivo* studies to exclude possible Cre toxicity (Silver and Livingston, 2001). Luxol fast blue with H&E staining from adult mice 3 months after *Igf2* removal revealed no gross anatomical changes in the brain structures surrounding the SVZ or SGZ of the *Igf2*-inducible KO (iKO) mice (Figures 1E and 1F). Additionally, no differences were observed in organ weights of the heart, lung, liver, kidney, and spleen adjusted to total body weight for WT and iKO mice (data not shown).

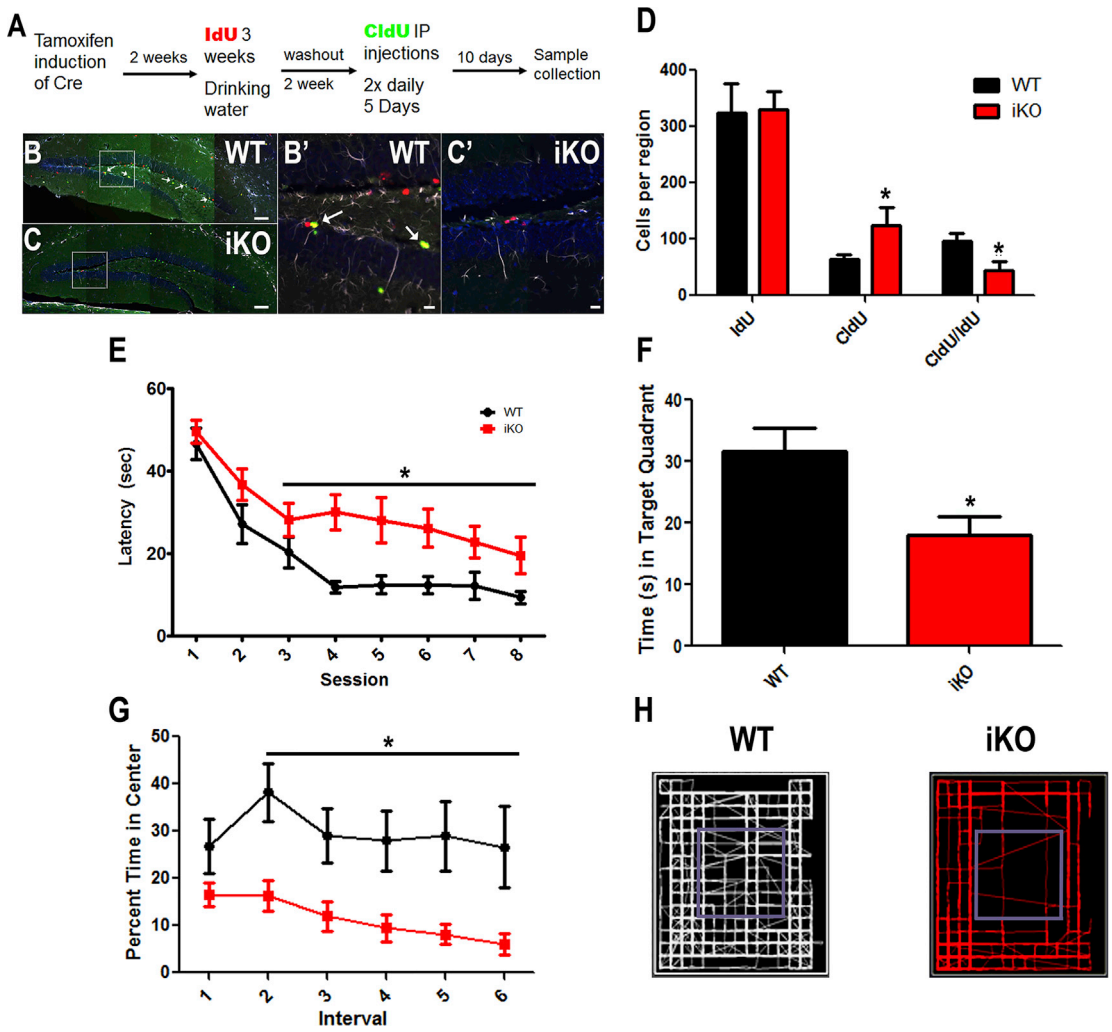

Figure 2. IGF-II Maintains Label-Retaining Cells in the SGZ of the Hippocampus and Is Necessary for Learning and Memory

Schematic of timeline for tamoxifen administration and labeling with IdU and CldU (A). Representative images of the hippocampi of WT (B) and iKO mice (C). Scale bars, 100 μm. IdU red, CldU green, GFAP white, and DAPI blue. (B′) and (C′) are insets from the regions marked in (B) and (C), respectively (scale bars, 20 μm). Counts of single- and double-positive cells for CldU and IdU in the SGZ (D), n = 6 WT and n = 6 iKO mice. See also Figures S2 and S3. Morris water maze latency to platform in seconds (E), and probe trial (F), n = 13 WT and n = 16 iKO mice. Open field test percent time spent in center across each 5-min interval (G), and maps of typical path taken (H), n = 10 WT and n = 15 iKO mice. WT black, iKO red. Statistical significance in (D) and (F) by Student's t test (*p < 0.05) and repeated-measures ANOVA in (E) and (G) (*p < 0.05). In (E), a session effect was observed in WT mice but not in iKO mice. Error bars represent SEM.

To evaluate the effects of *Igf2* deletion on NSCs and progenitors in the SGZ and SVZ, we analyzed the preservation of label-retaining cells using temporally spaced administrations of the thymidine analogs iododeoxyuridine (IdU) and chlorodeoxyuridine (CldU) as depicted in Figure 2A (Llorens-Martin and Trejo, 2011; Vega and Peterson, 2005). Studies were performed to validate lack of cross-reactivity in detecting IdU and CldU (Figure S2). We examined the number of IdU and CldU single- and double-positive cells in the SGZ and SVZ in the WT and iKO mice, where double analog-positive cells are the label-retaining, slowly cycling, NSCs (Figures 2 and 3). Glial fibrillary acidic protein (GFAP), which is expressed by adult NSCs in SVZ and SGZ, was also included for analysis. Triple-positive IdU/CldU/GFAP cells were observed in the SGZ and SVZ, along with IdU and CldU single-positive cells (Figures 2B–2C′ and 3A–3D′) but it was difficult to establish whether a cell was definitively $GFAP^+$ and thymidine analog positive; therefore, GFAP expression was not included in the stereology analyses. The numbers of single- and double-positive cells for the analogs were counted using unbiased stereology (Figures 2D and 3E). Significantly fewer $IdU^+/CldU^+$ cells

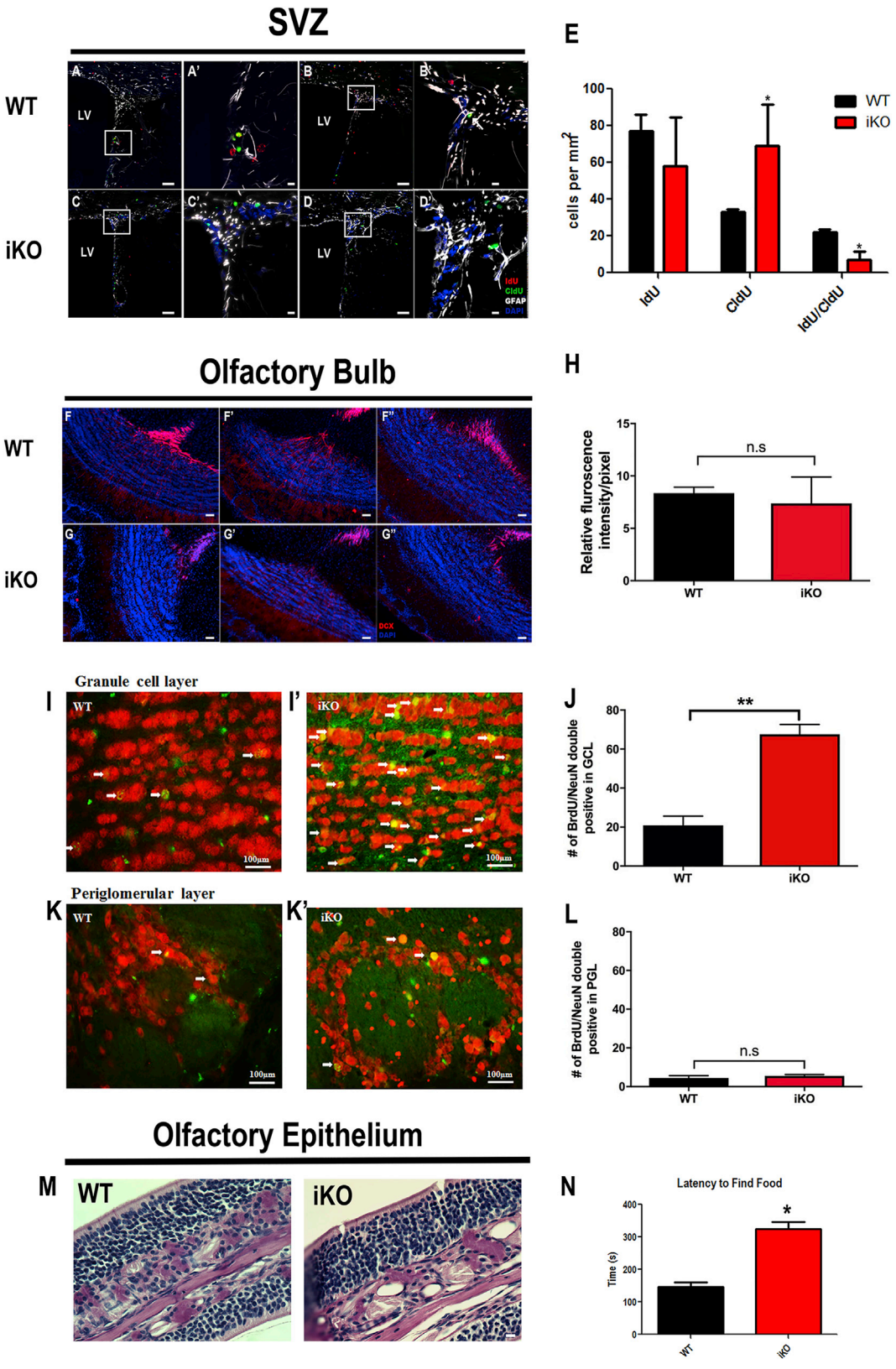

(legend on next page)

Table 1. Multicolor Flow Cytometry Reveals a Decrease in SVZ Neural Stem Cells after *Igf2* Conditional Deletion

Cell Type	NSC	MP1	MP2	GRP/MP3	MP4	PFMP	BNAP	GRP3
WT	1.27% ± 0.09%[a]	18.73% ± 2.53%	4.30% ± 1.30%	10.33% ± 1.40%	0.50% ± 0.31%	0.90% ± 0.23%	8.68% ± 1.90%	0.34% ± 0.07%
iKO	1.01% ± 0.07%*[b]	21.87% ± 2.02%	4.91% ± 1.46%	8.33% ± 1.30%	0.33% ± 0.21%	1.03% ± 0.19%	13.46% ± 2.30%	0.38% ± 0.06%

See also Figure S3. NSC, neural stem cell; MP1, multipotential 1; MP2, multipotential 2; MP3/GRP2, multipotential 3/glial restricted progenitor 2; PFMP, PDGF- and FGF-responsive multipotential progenitors; BNAP/GRP1, bipotential neuronal-astrocytic precursor/glial restricted progenitor 1; GRP3, glial restricted progenitor 3; WT, wild-type; iKO, inducible KO.

[a]Data are presented as mean values ± SEM, n = 17 WT and 19 iKO mice of both sexes.

[b]*p < 0.05 by one-way ANOVA and Tukey's post hoc test.

were observed in both the SGZ (Figure 2D) and SVZ (Figure 3E) in the iKO mice compared with WT mice, consistent with an essential function for IGF-II in NSC homeostasis. Concomitant with the loss of $IdU^+/CldU^+$ cells, there was an increase in progenitors that were only $CldU^+$ in the iKOs attributable to maturation of NSCs into progenitor cells (Figures 2D and 3E). Using a four-color flow-cytometry panel established in the Levison lab (Buono et al., 2012, 2015a), we evaluated the composition of the SVZ 12 months after Cre induction. Compared with the controls there was a statistically significant reduction in the NSCs (1.27% ± 0.09% NSCs in WT versus 1.01% ± 0.07% in iKOs) with modest increases in the proportions of two progenitor cell populations (Table 1). We evaluated the extent of apoptotic death within the SVZ and SGZ using *in situ* end labeling but detected no difference between the WT and iKO mice, indicating it was unlikely that the decrease in IdU/CldU-labeled cells in the iKO mice was due to apoptotic cell death (Figure S3).

Several studies have correlated increased or decreased cell proliferation in the SGZ with improvements or deficits in learning and memory, respectively (for a review see Zhao et al., 2008). Since *Igf2* deletion altered the numbers of dual nucleotide label-retaining cells and increased the number of $CldU^+$ proliferating cells, we performed studies to determine whether the *Igf2* iKO mice had deficits in hippocampal function using the Morris water maze to test spatial learning and memory and the open field test to evaluate exploratory activity and anxiety (Figures 2E–2H). WT mice initially required 50 s to find the hidden platform in the Morris water maze, but quickly learned the location of the platform, and their latency to find the platform decreased from 50 s to 10 s. By contrast, the iKO mice were impaired in learning and displayed longer latencies to find the platform (repeated-measures ANOVA, n = 16 iKO and n = 13 WT) (Figure 2E). To test memory retention, we tested mice in a probe trial. WT mice swam significantly longer (50%) in the target quadrant than the iKO mice (35%) (Figure 2F). There was no difference between genotypes in the ability to find a visible platform (data not shown).

We further assessed the effects of losing IGF-II on exploratory and anxiety behavior using an open field test. Mice were placed into an open field test apparatus and were evaluated across six 5-min intervals. Overall the total distance traveled was unaltered between WT and iKO mice (data not shown). However, the iKO mice traveled less distance than the WT mice in the first two intervals (iKO 1,683 ± 121 and 1,103 ± 104 versus WT 2,072 ± 129 and 1,426 ± 94), and the total time that the iKO mice were immobile was significantly increased compared with WT mice (iKO 955.4 ± 47.7 versus WT 761 ± 64.8). What emerged most clearly across trials was that the iKO mice avoided the center of the arena (Figures 2G and 2H) (n = 13 iKO and n = 10 WT), indicating increased anxiety in the iKO mice.

Figure 3. IGF-II Is Required for SVZ NSC Maintenance, OB Neurogenesis, and Olfaction

WT (A and B) and iKO (C and D) mouse SVZs stained for IdU, CldU, and GFAP; insets (with primes) are enlargements. Scale bars, 100 μm (A–D) and 20 μm (A′–D′). IdU red, CldU green, GFAP white, and DAPI blue. Counts of single- and double-positive cells for CldU and IdU within 20 μm of the lateral ventricle wall (E), n = 6 WT and n = 6 iKO mice. See also Figures S2 and S3. Olfactory bulb was examined for immature neurons using doublecortin (DCX, red) and DAPI (blue) in WT (F) and iKO (G). Scale bars, = 100 μm. Fluorescence intensity was measured for DCX^+ cells (H), n = 3 WT and n = 3 iKO mice. WT (I and K) and iKO (I′ and K′) for granule cell layer (I and I′) and periglomerular layer (K and K′) stained for BrdU and NeuN, 5 weeks after administering BrdU. Arrows indicate double-positive, newly generated neurons. Scale bars, 100 μm. Quantification of newly formed cells in the granule cell layer (J) and periglomerular cell layer (L), n = 3 WT and n = 3 iKO mice. See also Figure S4. Paraformaldehyde fixed and decalcified preparations of mouse nasal pharynxes were embedded in paraffin and sectioned at 8 μm. Sections from WT and iKO mice were stained using PAS and visualized by light microscopy; representative sections of WT and iKO mice are provided. Scale bar, 20 μm (M). Buried food test showing latency to find food versus genotype (N), WT (black) and iKO (red), n = 5 WT and n = 6 iKO mice. Statistical significance: *p < 0.05 and **p < 0.005 using Student's t test, iKO versus WT. Error bars represent SEM.

One function of the NSCs in the rodent SVZ is to give rise to neuroblasts that migrate through the rostral migratory stream (RMS) to the olfactory bulb, resulting in 10,000–30,000 new neurons per day (Lledo and Saghatelyan, 2005). As the iKO mice had fewer $IdU^+/CldU^+$ cells but increased $CldU^+$ cells in the SVZ, we performed analyses to determine whether there were increased numbers of migrating neuroblasts or new neurons in the olfactory bulb. The relative numbers of doublecortin (DCX)-positive immature neurons in the RMS entering the olfactory bulb were equivalent between the WT and iKO mice (Figures 3F–3H). However, using bromodeoxyuridine (BrdU) to label dividing progenitors in the SVZ and $BrdU^+/NeuN^+$ immunostaining to trace their differentiation into new olfactory bulb neurons, we observed a dramatic increase in the number of double-positive BrdU/NeuN cells in the granule cell layer of the olfactory bulb in the iKO mice compared with the WT mice (Figures 3I and 3J). In contrast, the number of double-positive BrdU/NeuN cells was unchanged in the iKO periglomerular layer of the olfactory bulb (Figures 3K and 3L). It has been well established that the new olfactory bulb neurons produced by the SVZ are GABAergic inhibitory interneurons (Betarbet et al., 1996; Carleton et al., 2003; Kato et al., 2001; Petreanu and Alvarez-Buylla, 2002; Winner et al., 2002); however, we were unsuccessful in establishing which subset of interneurons were overproduced as neither calretinin, calbindin, nor tyrosine hydroxylase stained the $BrdU^+/NeuN^+$-labeled neurons (Figure S4).

Using the buried food test as an olfaction assay, we found that the iKO mice took twice as long as the WT mice (iKO 325 ± 24 s versus WT 146 ± 18 s) to find a buried Fruit Loop (Figure 3N). As there are stem cells and olfactory receptor cells in the olfactory epithelium that turn over, an involution of the olfactory epithelium could explain the olfaction deficit; however, the morphology and structure of the olfactory epithelium appeared unchanged in both H&E-stained and periodic acid-Schiff (PAS)-stained sections of the iKO mice (Figure 3M). Therefore, we conclude that the loss of IGF-II led to an increase in SVZ progenitors, which in turn led to the overproduction of new inhibitory neurons in the olfactory bulb, resulting in a deficit in olfaction.

Adult ISCs Require Sustained IGF-II Production

We next asked whether IGF-II has a broader function in maintaining other adult stem cells. We speculated that the lethality of *Igf2* iKO mice receiving five consecutive daily doses of tamoxifen might be due to a rapid loss of ISCs, whose differentiated progeny normally live for 3–5 days after cell-cycle exit (van der Flier and Clevers, 2009). To test this hypothesis, we analyzed the intestines from tamoxifen-injected iKO mice and their WT littermate controls on day 6 after tamoxifen administration. At this time, there was an average of 15% body-weight loss in iKO mice when compared with the WT littermates (Figure 4A). Analyses of the chemical composition of the plasma failed to detect consistent differences between the iKOs and WT mice; hematocrit was normal in iKOs, and no difference was detected in leukocyte frequencies (data not shown). However, iKO mice showed clear signs of declining health including hunched backs, lethargy, and reduced food/water intake (data not shown). All iKOs, if not sacrificed at this time, would die within a week. The intestinal tract of the iKO mice appeared translucently pale with dilated lumen, enlarged cecum, and no solid feces in the colonic lumen (Figures 4B–4E). These pathological effects were not due to tamoxifen toxicity, as intestines from the WT littermates subjected to the identical tamoxifen treatment appeared normal.

In situ hybridization showed that *Igf2* was highly expressed in WT crypts and at lower levels in villus epithelium as well as some mesenchymal cells (Figures 4F, 4F′, and 4H). *Igf2* mRNA levels were significantly reduced in iKO intestines (Figures 4G–4H). Immunohistochemistry for IGF-II confirmed the mRNA pattern with IGF-II protein drastically reduced in iKO intestines, most notably in the crypts (Figures 4I–4K).

Histological examination suggested a clear loss of villus-crypt boundaries and a transit amplifying cell zone in iKO intestines, where the villi became severely blunted (Figures 5A–5B′). Approximately 80% of the WT crypts had robust expression of Olfm4, a marker of crypt-based columnar (CBC) stem cells (Barker et al., 2007; van der Flier and Clevers, 2009), whereas only 10% of the iKO crypts showed detectable *Olfm4* expression (Figures 5C–5E). Even when $Olfm4^+$ crypts were occasionally found, these crypts had an abnormal morphology (Figure 5D, inset). $Ki67^+$ transit amplifying cells were abundant in WT crypts but were significantly decreased in iKO crypts (Figures 5F–5H), suggesting that loss of IGF-II caused a severe reduction of transit amplifying and potentially stem/progenitor cell populations.

Lysozyme-positive Paneth cells were present at the bottom of the WT crypts (Figures 5I, 5I′, and 5K). In contrast, all Paneth cells were virtually eliminated from the iKO crypts (Figures 5J, 5J′, and 5K). Some $lysozyme^+$ cells were seen in the iKO villi (Figures 5J [arrowhead and inset], 5J′, and 5K). qRT-PCR verified an overall reduction of the genes in the iKO that are characteristic of Wnt/β-catenin signaling and fast-cycling stem cells (Figures 5L and 5M), as well as Paneth cells (Figure 5N) and alternative stem cell populations (Figure 5O). These data suggested that there was a severe impairment in the crypt compartment affecting both stem and Paneth cell populations in iKO mouse intestines.

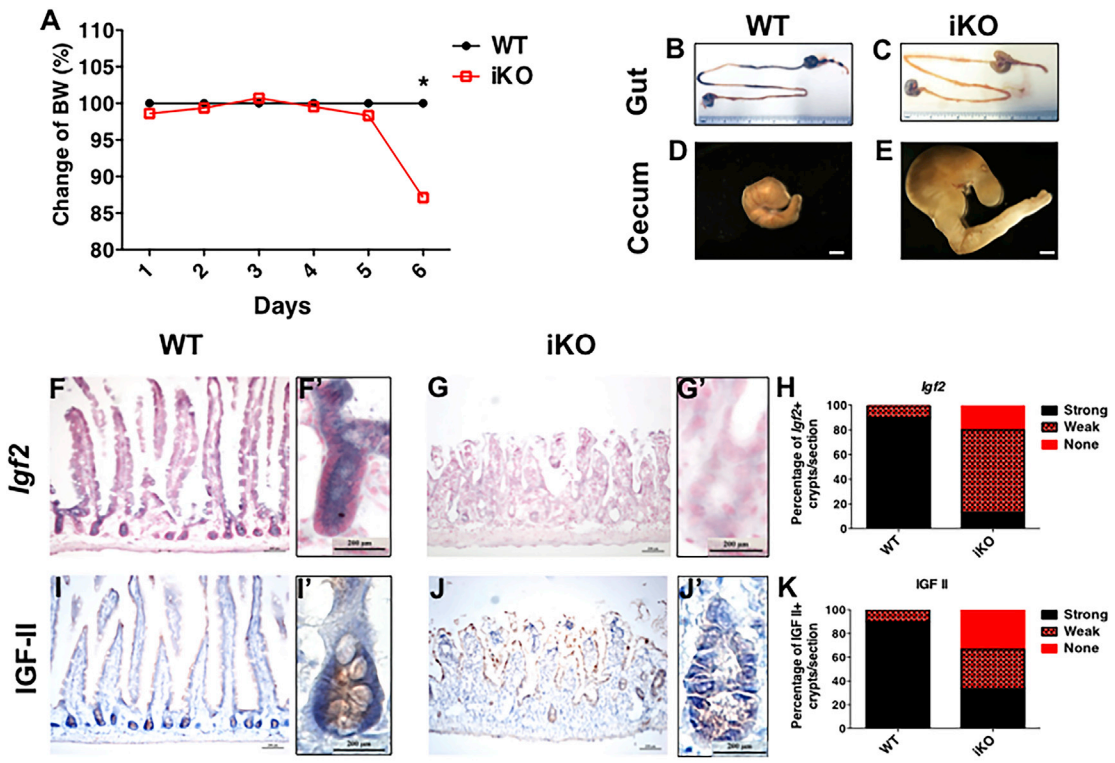

Figure 4. Loss of IGF-II Abrogates Intestinal Homeostasis

Five consecutive injections of tamoxifen (75 mg/kg) were administered from day 1 to day 5 and tissues were analyzed on day 6. Body-weight curve of WT and iKO mice from day 1 to day 6 (A), n = 3 WT and n = 4 iKO mice. WT (B and D) and iKO (C and E) guts were surgically dissected (from the stomach to the colon) and the ceca were photographed at day 6. Scale bars, 6 inches for intestines and 200 μm for cecum. *Igf2* mRNA (F–G′) and IGF-II protein (I–J′) levels were detected in WT (F, F′, I, and I′) and iKO (G, G′, J, and J′) intestine using *in situ* hybridization and immunohistochemistry, respectively. Scale bars, 200 μm. n = 3 WT and n = 3 iKO mice. *$p < 0.05$ by Student's t test. Error bars represent SEM.

To determine whether ISCs in iKO crypts indeed lost self-renewal capacity, we isolated intestinal crypts from WT and iKO mice 5 days after tamoxifen administration *in vivo*, and cultured them in EGF, Noggin, and R-spondin-1 (ENR) medium. WT crypts underwent continuous budding (Figure 6A), whereas few iKO crypts initiated budding (arrows in Figure 6A). The percentage of viable iKO organoids was significantly reduced (Figure 6B). We then performed inducible *Igf2* deletion in culture, by adding 4-hydroxytamoxifen (4-OHT) to the iKO organoids that already formed *in vitro*. Addition of 4-OHT, but not vehicle, led to clear regression of buds in iKO organoids at day 3 (compare left and middle columns in Figure 6C). Tamoxifen-induced genomic recombination at *Igf2* locus was verified by PCR (Figure 6D). When we supplemented the ENR medium with IGF-II, such bud regression was prevented (right column in Figure 6C), even though similar recombination occurred in the organoid (Figure 6D). Counting of normal-appearing budding organoids from these cultures indicated a rescuing effect by the exogenous IGF-II protein (Figure 6E). 5-Ethynyl-2′-deoxyuridine (EdU) incorporation further suggested that 4-OHT treatment decreased numbers of the proliferative cells in epithelial buds, which was restored by IGF-II addition (Figures 6F and 6G). These data collectively demonstrate that IGF-II loss reduces the clonogenic activity of ISCs, supporting the idea that IGF-II is essential for adult ISC maintenance.

DISCUSSION

Taken altogether, our studies demonstrate that IGF-II is necessary for the maintenance of distinct adult epithelial stem cells in both the SVZ and SGZ of the brain and in the intestine, thus making it an essential factor for these stem cell niches. In these studies we removed *Igf2* from adult mice using two different tamoxifen dosing schemes, one time a day for 5 days or one time every 3 days across 15 days. Both dosing schemes significantly reduced levels of IGF-II; however, acutely deleting *Igf2* resulted in death

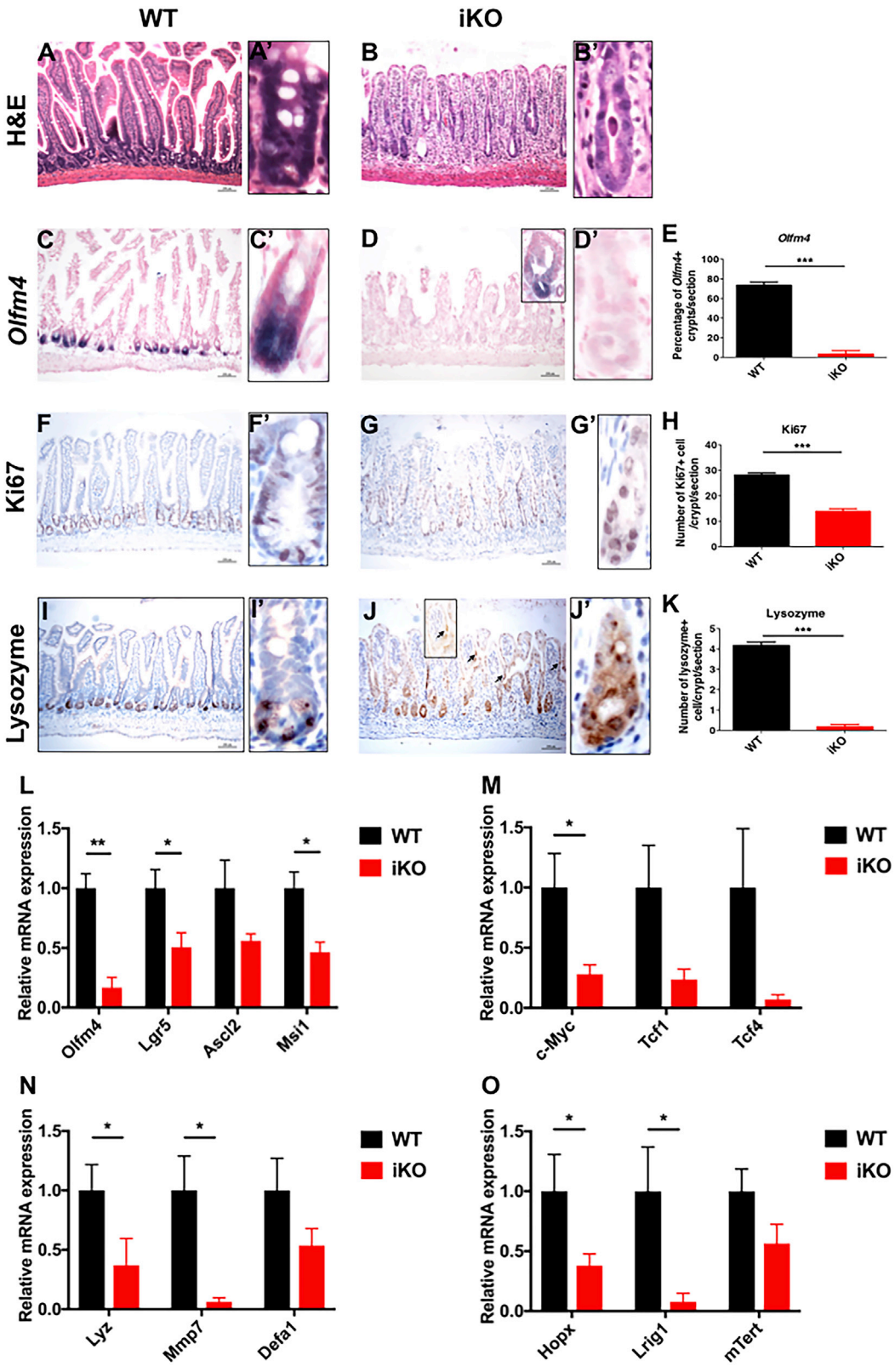

(legend on next page)

of the mice and, therefore, could only be used for short-term studies and not for long-term neurogenesis studies. The stem cells and proliferating progenitors in the intestinal crypt failed to self-renew, lethally compromising the functions of the gastrointestinal tract. Within a crypt, two stem cell populations have been described: fast-cycling and quiescent stem cells, and specific markers are available for their identification. Lgr5 and Olfm4 mark the fast-cycling or CBC stem cells, whereas Hopx, Bmi1, and Lrig1 mark the quiescent stem cells (Barker et al., 2007; Sangiorgi and Capecchi, 2008; Takeda et al., 2011; Yin et al., 2014). Under certain conditions (e.g., injury, radiation), interconversion between the two stem cell populations has been reported, although the functional significance of the quiescent stem cells remains under debate given the robust expression of all quiescent stem cell markers by $Lgr5^+$ cells (Porter et al., 2002; Sato et al., 2011). When ISCs were examined using the same tamoxifen administration protocol as used to study the NSCs (five doses of tamoxifen administered every 3 days), little effect was observed. The small intestines in the iKO mice appeared normal upon gross inspection. However, there was a significant increase in the $Ki67^+$ transit amplifying cell population ($p < 0.001$), and a slight but nonsignificant increase in crypts with multiple $Hopx^+$ cells (Figure S5). These results suggest that slow deletion of *Igf2* allowed alternative intestinal epithelial cell populations, as we recently reported (Yu et al., 2018), to compensate for the loss of fast-cycling stem cells, which appear to be more sensitive to IGF-II loss.

Igf2 deletion reduced the numbers of dual nucleotide label-retaining cells and increased newly dividing cells labeled for the second nucleotide (CldU) in both the SGZ and SVZ, which correlated with behavioral deficits in the Morris water maze, open field test, and the buried food test. Our findings taken together with the prior studies by Bracko et al. (2012) and Ferron et al. (2015) now reveal that IGF-II regulates adult NSCs in both the SVZ and SGZ, but that distinct sources of IGF-II support these two neurogenic niches. In the SGZ/DG, *Igf2* is expressed by the NSCs themselves, and this autocrine production is likely the main source of IGF-II for the NSCs. Ferron et al. (2015) demonstrated that *Igf2* deletion from the endothelial compartment has little impact on the SGZ/DG NSCs. In the SVZ, the main sources of IGF-II that regulate the NSCs likely are from both the choroid plexus and endothelial cells (Ferron et al., 2015; Lehtinen et al., 2011). The complete deletion of *Igf2* in the adult brain in our study resulted in a reduction in the SGZ/DG and SVZ NSCs and likely contributed to the greater effect we saw on the neurogenic niches that resulted not only in a reduction in NSC numbers but also in an increase in rapidly dividing progenitors. Moreover, we observed a burst of newly generated neurons in the olfactory bulb. Whereas embryonic deletion of *Igf2* caused a reduction in NSCs in both adult niches, Ferron et al. (2015) saw no concomitant increase in rapidly dividing progenitors or in newly generated neurons in the olfactory bulb in these mice or in mice with endothelial *Igf2* deletion. It is possible that the embryonic deletion of *Igf2* significantly altered the initial establishment of NSCs present in the adult SVZ, consistent with the significant reduction in brain size in these mice.

Several studies have begun to establish a link between IGF-II, memory, and cognitive impairment. For example, IGF-II in the hippocampus is necessary for memory consolidation and promotes memory enhancement (Alberini and Chen, 2012; Chen et al., 2011). Moreover, IGF-II is being considered as a therapeutic target for Alzheimer's disease (Mellott et al., 2014). Our studies demonstrating that IGF-II is required for maintenance of a subset of adult NSCs suggest that IGF-II may be important for healthy aging and that reduced levels of IGF-II that occur with aging (Bartke et al., 2003; Chen et al., 2008; Kelijman, 1991) may contribute to neurodegenerative or psychiatric diseases.

Our studies demonstrating that IGF-II also is essential for the rapidly dividing ISCs has important implications for understanding the regulation of epithelial stem cell renewal in the intestines as well as for understanding and treating colorectal cancers. The rapid deletion of *Igf2* impaired ISC homeostasis, as manifested by loss of CBCs and transit amplifying cells. This phenotype was strong in all iKO mice that received five consecutive doses of tamoxifen. The lethality and the histopathology are reminiscent of Tcf4 deletion (Korinek et al., 1998; van Es et al., 2012), conditional deletion of β-catenin (Fevr et al., 2007; Ireland et al., 2004), or overexpression of secreted *Dickkopf-1*, a Wnt inhibitor (Kuhnert et al., 2004; Pinto et al., 2003). Redundancy exists among various Wnt proteins, and there are multiple sources of Wnts in the intestinal stem cell niche (Aoki et al., 2016; Farin et al., 2012; Kabiri et al., 2014). In contrast, the phenotype presented here that resulted from the loss of a single growth factor, IGF-II, was striking.

Figure 5. IGF-II Maintains the Morphology and Stemness of the Small Intestine

Small intestine of WT and iKO mice after five consecutive injections of tamoxifen (75 mg/kg) were stained and quantified for H&E (A–B′), *Olfm4* (C–E), Ki67 (F–H), and lysozyme (I–K). qPCR analyses were performed in WT and iKO intestines to detect marker genes for stem cells (L), progenitors (M), Paneth cells (N), and quiescent stem cells (O). n = 3 (WT) and 3 (iKO) mice. See also Figure S5. Scale bars, 200 μm. * $p < 0.05$, ** $p < 0.01$, *** $p < 0.001$ by Student's t test. Error bars represent SEM.

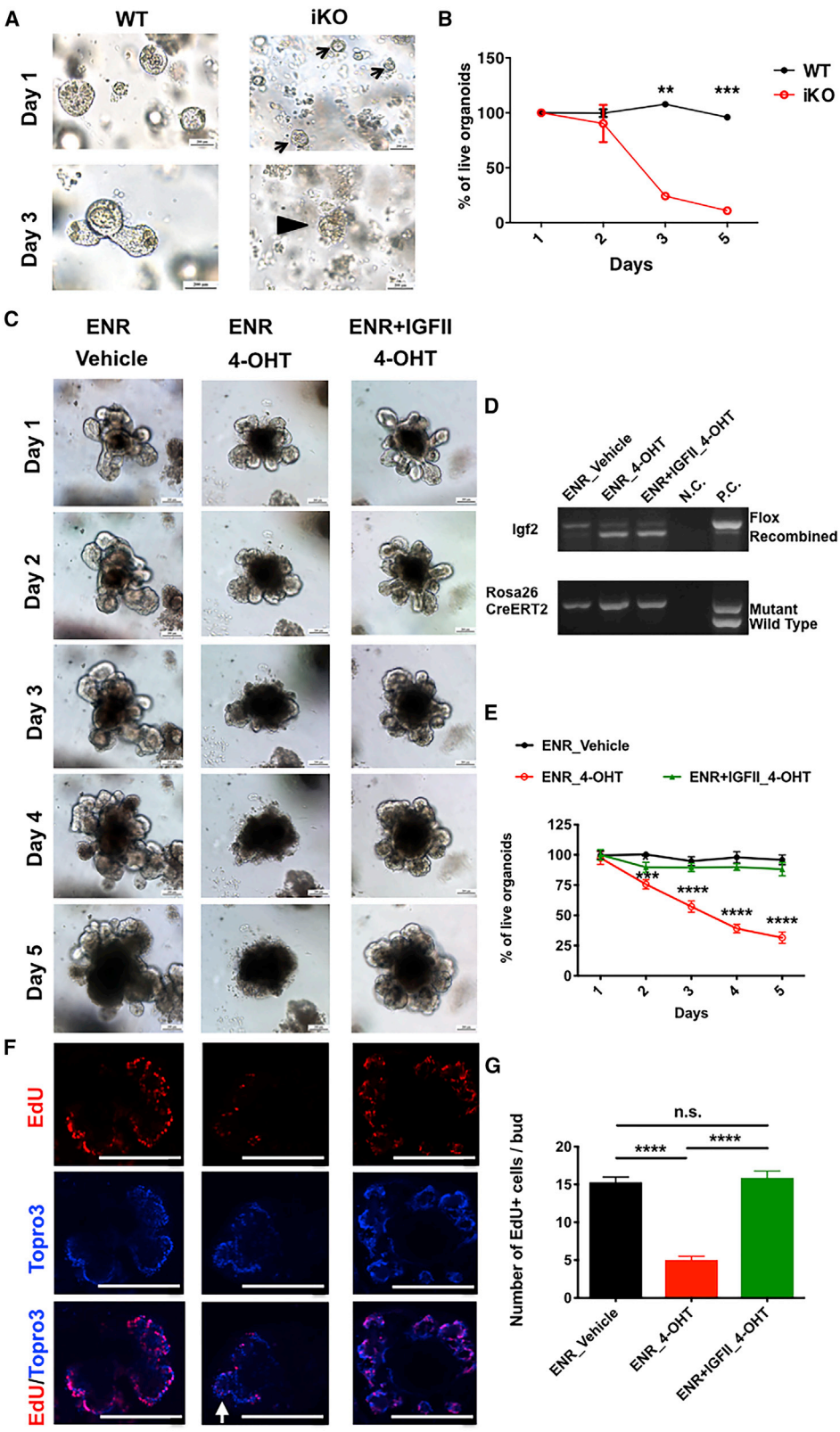

(legend on next page)

LOI of *Igf2* is found commonly in many types of cancer, including colorectal cancer (CRC) (Gelato and Vassalotti, 1990; Lamonerie et al., 1995; Yee et al., 1988), and *Igf2* LOI is a potential marker for CRC risk (Cui et al., 2003). Increased allelic *Igf2* expression promotes intestinal tumor formation and hyperproliferation of crypt epithelium with longer intestinal crypts (Bennett et al., 2003; Harper et al., 2006). Overexpression of *Igf2* shifts cells to a less differentiated state, resulting in increased tumor initiation rather than proliferation (Sakatani et al., 2005). Insulin receptor substrate 1 (IRS-1), which is an intracellular mediator of both insulin and the IGF actions, has been implicated as an important determinant for ISC survival after injury, and partial or absolute IRS-1 deficiency in mice carrying the $Apc^{min/+}$ mutation led to reduced tumor number relative to IRS-$1^{+/+}$/$Apc^{min/+}$ mice. Furthermore, elevated levels of insulin correlate with both low intestinal epithelial cell apoptosis and increased adenoma risk (Keku et al., 2005; Ramocki et al., 2008).

Our prior published studies indicate that IGF-II promotes SVZ NSC stemness *in vitro* through the A splice isoform of the insulin receptor and independently of either the IGF type 1 receptor (IGF-1R) or IGF-2R (Ziegler et al., 2012, 2014). Interestingly, the recent study by Bracko et al. (2012) showed that IGF-II acted through the IGF-1R to support DG/SGZ NSCs. Thus, IGF-II may have specific effects on the two neurogenic niches through distinct receptors to promote cell regeneration and healthy aging. While structurally similar, the differences in the biological effects of IGF-I and IGF-II are significant, and our studies demonstrate that much more needs to be learned about IGF-II and how it signals through its cognate receptors to affect specific adult stem cell populations.

EXPERIMENTAL PROCEDURES

Animals

All experiments were performed in accordance with protocols approved by the institutional animal care and use committee of Rutgers-New Jersey Medical School and in accordance with the National Institutes of Health Guide for the Care and Use of Laboratory Animals (NIH Publications No. 80-23) revised in 1996. Mouse strains included Cre^{ER} driven off a Gt(*ROSA*)26Sor promoter (Gt(ROSA)26$Sor^{tm1(cre/Esr1)Nat}$/J) (Jax mouse stock #004847) and floxed *Igf2* mice (Haley et al., 2012). Mice were obtained as C57BL/6 mixed strain and were backcrossed for five generations onto C57BL/6 (Jackson Laboratory) prior to use. Male and female mice, heterozygous for Cre, Gt(ROSA)26$Sor^{tm1(cre/Esr1)Nat}$/J and homozygous for floxed *Igf2* were bred to generate mice used for the experiments. Progeny from the cross consisted of either heterozygous or homozygous Cre with homozygous floxed *Igf2* (iKO) and homozygous floxed *Igf2* mouse littermates that did not carry the Cre (WT).

Tamoxifen and Nucleotide Administration

Both Cre^{+} (iKO) and Cre^{-} (WT) mice were administered tamoxifen (Sigma T5648; 75 mg/kg) intraperitoneally beginning at 4–5 weeks of age according to the schedule in Figure 1 for the NSC analyses or over 5 consecutive days for the intestinal analyses. For the NSC analysis, mice were 54 days old (±5 days) at the start of dual analog labeling and approximately 6 months old at tissue collection, and were the same across genotypes. A distinct cohort of mice between the ages of 2.5 and 6 months were used for behavioral studies. For the ISC analyses, mice were used 5–6 days following administration of tamoxifen.

Thymidine Analog Detection

IdU (Sigma I7125) or BrdU (Sigma, B5002) were provided at 1 mg/mL in 1% sucrose water. CldU (Sigma C-6891), dissolved in 0.9% saline, was administered intraperitoneally at 42.5 mg/kg. IdU and CldU detection was performed as described by Tuttle et al. (2010). GFAP (DAKO 1:500) was also included for analysis. IdU was detected with Dylight 549 conjugated secondary antibody, CldU with Dylight 488 conjugated secondary antibody, and GFAP with an Alexa 647 conjugated secondary antibody (all from Jackson ImmunoResearch) along with 4′,6′-diamidino-2-phenylindole (DAPI) at 1:1,000 in PBS for 15 min. Slides were coverslipped using Fluorogel (Electron Microscopy Sciences, #19440).

Stereology

For stereology analysis, 8-μm adjacent hippocampal or 5-μm adjacent SVZ tissue sections stained with CldU/IdU/GFAP/DAPI were used. Cell counts were performed using the physical fractionator (StereoInvestigator; MBF Bioscience). A systematic random sampling of cells within the regions of interest in adjacent sections was performed bidirectionally to obtain an unbiased estimate of the number of single-, double-, and triple-labeled cells. Sections were coded to ensure blinding during image acquisition and counting.

DCX, NeuN, and *In Situ* End Labeling Staining

DCX staining was performed using a goat polyclonal anti-DCX (1:100, Santa Cruz Biotechnology SC 8066) as previously described

Figure 6. *Igf2* Knockout Impairs the Growth of Intestinal Organoids

WT and iKO ($Igf2^{fl/fl}Cre^{+/-}$) organoids were cultured in medium containing EGF, Noggin, and R-spondin1 (ENR) for 5 days. Arrows delineate small organoids with few Paneth cells. Arrowhead indicates dying organoid on day 3, which was confirmed to be dead on day 5 (A). Survival curve of organoids from WT and iKO mice (B). 4-OHT or vehicle was added to iKO ($Igf2^{fl/fl}Cre^{+/+}$) organoid cultures at day 7. The organoids were imaged daily (C), harvested for genotyping (D), and scored daily (E). The positive control (p.c.) used in (D) is the genomic DNA sample from a Rosa26-CreER heterozygous mouse sample to show the WT (bottom) and mutant (upper) PCR products. EdU staining was performed at day 4 after 4-OHT treatment (F and G). Scale bars, 200 μm. *$p < 0.05$, **$p < 0.01$, ***$p < 0.001$ versus controls by Student's t test or one-way ANOVA. Data were analyzed from n = 3 independent mice. Error bars represent SEM.

(Yang et al., 2008). The relative fluorescence intensity of DCX-positive cells was quantified using ImageJ software. Sections were stained for BrdU and NeuN as described previously (Goodus et al., 2015). *In situ* end labeling was performed as described previously (Romanko et al., 2004). Images were taken using a Q-imaging mono 12-bit camera interfaced with iVision 4 scientific imaging software (Scanalytics).

For multicolor flow cytometry, WT and iKO mice were administered tamoxifen (75 mg/kg) every 3 days beginning at 4–5 weeks of age and were euthanized at 12 months of age. SVZ cells were dissociated and stained using fluorescently labeled probes to the following cell-surface antigens: CD133/LeX/NG2/CD140a. A total of 50,000 cell events were analyzed per animal after excluding debris and dead cells by DAPI. A two-gate strategy was used to group cells into one of eight categories.

Behavioral Tests

Mice were tested for alterations in olfaction using a buried food test as described by Yang and Crawley (2009). Deficits in hippocampal function were determined using the Morris water maze to test spatial learning and memory and the open field test to evaluate exploratory activity and anxiety (for a review see Zhao et al., 2008). Details of these procedures can be found in Supplemental Experimental Procedures.

Intestinal Tissue Analyses

Small intestines were dissected and flushed with cold PBS. The proximal halves were fixed in DEPC-treated 4% paraformaldehyde for 1 h at room temperature, changed into 30% sucrose overnight at 4°C, frozen, and sectioned at 10 μm for *in situ* hybridization. The distal halves were fixed in 4% paraformaldehyde overnight, embedded in paraffin, and sectioned at 5 μm for immunohistochemistry. *In situ* hybridization analysis for *Igf2* and *Olfm4* was performed as previously described (Gregorieff and Clevers, 2010; Gregorieff et al., 2005). Paraffin sections were stained with H&E, for lysozyme (1:8, Biogenex), Ki67 (1:2000, Vector Laboratories), and Hopx (1:1,000, Santa Cruz). Frozen tissue sections were stained for IGF-II (1:1,000, Santa Cruz) as previously described (Gao et al., 2009). For *Igf2 in situ* hybridization and IGF-II immunohistochemistry, individual crypts were visually scored, based on staining intensities, into none, weak, and strong categories. Percentage of each category was presented in results. For Olfm4 *in situ*, crypts with positive Olfm4 staining were manually counted and reported from sections of intestinal tissues. For Ki67, lysozyme, and EdU staining, numbers of positive cells were counted for individual crypts and reported as the average number per crypt. For Hopx, percentages of crypts containing 1, 2, or 0 strongly Hopx-positive cells were reported. All values are presented as means ± SEM. Differences among groups were analyzed by Student's t test with GraphPad Prism version 5.01. Significance was noted when p was less than 0.05.

Intestinal Organoid Culture

Organoids were derived from isolated crypts of the proximal small intestine of WT and iKO mice as described previously (Sato and Clevers, 2013; Sato et al., 2009). Organoids were maintained in an ENR-containing medium. Organoid growth was imaged and quantified by scoring the number of live organoids that developed during the 5 days after isolation or treatment. For *in vitro* induction of *Igf2* deletion, organoids were derived and cultured as above from iKO ($Igf2^{fl/fl}Cre^{+/+}$) mice and were treated for 12 h with either 0.5 μM 4-OHT (iKO) or vehicle on day 7 as described previously (Farin et al., 2012). EdU (Life Technologies) staining was performed according to the manufacturer's instructions. Data were analyzed from organoids isolated from three independent mice.

SUPPLEMENTAL INFORMATION

Supplemental Information can be found online at https://doi.org/10.1016/j.stemcr.2019.02.011.

AUTHOR CONTRIBUTIONS

A.N.Z. collected and analyzed neural stem cell data; Q.F. collected intestinal stem cell data; J.M.T. performed and analyzed Morris water maze studies; M.C. and I.S. generated floxed *Igf2* mice; S.C., E.K., and D.E.R. performed and analyzed the BrdU/NeuN immunostaining experiments; T.C. and K.P. contributed to behavioral study designs and data analysis; Q.F. and N.G. analyzed intestinal data; A.N.Z., S.W.L., and T.L.W. designed the studies of NSCs; A.N.Z., Q.F., N.G., S.W.L., and T.L.W. wrote the manuscript. All authors discussed the results, provided comments on drafts, and approved the final manuscript.

ACKNOWLEDGMENTS

This work was supported by NIH National Institute on Neurological Disorders and Stroke R21NS076874 awarded to S.W.L and T.L.W., and F31NS065607 awarded to A.N.Z., NIH National Institute of Diabetes and Digestive and Kidney Diseases R01DK102934 awarded to N.G., NIH National Cancer Institute R21CA178599 awarded to N.G., American Cancer Society RSG-15-060-01-TBE awarded to N.G., and Medical Research Council (United Kingdom) MRC MC UU 12012/4 awarded to M.C.. Q.F. received a postdoctoral fellowship from the New Jersey Commission on Cancer Research (DFHS16PPC045). The authors would like to thank Dr. Robert Smith for sharing an important insight during a discussion at the IGF Gordon Conference. The authors also thank Dr. Eldo Kuzikandathil for use of his open field apparatus, and Dr. Soumya Das and Dr. Shiyan Yu for providing reagents.

Received: April 29, 2015
Revised: February 19, 2019
Accepted: February 20, 2019
Published: March 21, 2019

REFERENCES

Alberini, C.M., and Chen, D.Y. (2012). Memory enhancement: consolidation, reconsolidation and insulin-like growth factor 2. Trends Neurosci. *35*, 274–283.

Aoki, R., Shoshkes-Carmel, M., Gao, N., Shin, S., May, C.L., Golson, M.L., Zahm, A.M., Ray, M., Wiser, C.L., Wright, C.V., et al. (2016). Foxl1-expressing mesenchymal cells constitute the intestinal stem cell niche. Cell. Mol. Gastroenterol. Hepatol. *2*, 175–188.

Badea, T.C., Wang, Y., and Nathans, J. (2003). A noninvasive genetic/pharmacologic strategy for visualizing cell morphology and clonal relationships in the mouse. J. Neurosci. *23*, 2314–2322.

Baker, J., Liu, J.P., Robertson, E.J., and Efstratiadis, A. (1993). Role of insulin-like growth factors in embryonic and postnatal growth. Cell *75*, 73–82.

Barker, N., van Es, J.H., Kuipers, J., Kujala, P., van den Born, M., Cozijnsen, M., Haegebarth, A., Korving, J., Begthel, H., Peters, P.J., et al. (2007). Identification of stem cells in small intestine and colon by marker gene Lgr5. Nature *449*, 1003–1007.

Bartke, A., Chandrashekar, V., Dominici, F., Turyn, D., Kinney, B., Steger, R., and Kopchick, J.J. (2003). Insulin-like growth factor 1 (IGF-1) and aging: controversies and new insights. Biogerontology *4*, 1–8.

Bennett, W.R., Crew, T.E., Slack, J.M., and Ward, A. (2003). Structural-proliferative units and organ growth: effects of insulin-like growth factor 2 on the growth of colon and skin. Development *130*, 1079–1088.

Betarbet, R., Zigova, T., Bakay, R.A., and Luskin, M.B. (1996). Dopaminergic and GABAergic interneurons of the olfactory bulb are derived from the neonatal subventricular zone. Int. J. Dev. Neurosci. *14*, 921–930.

Bracko, O., Singer, T., Aigner, S., Knobloch, M., Winner, B., Ray, J., Clemenson, G.D., Jr., Suh, H., Couillard-Despres, S., Aigner, L., et al. (2012). Gene expression profiling of neural stem cells and their neuronal progeny reveals IGF2 as a regulator of adult hippocampal neurogenesis. J. Neurosci. *32*, 3376–3387.

Bunn, R.C., King, W.D., Winkler, M.K., and Fowlkes, J.L. (2005). Early developmental changes in IGF-I, IGF-II, IGF binding protein-1, and IGF binding protein-3 concentration in the cerebrospinal fluid of children. Pediatr. Res. *58*, 89–93.

Buono, K.D., Goodus, M.T., Guardia Clausi, M., Jiang, Y., Loporchio, D., and Levison, S.W. (2015a). Mechanisms of mouse neural precursor expansion after neonatal hypoxia-ischemia. J. Neurosci. *35*, 8855–8865.

Buono, K.D., Goodus, M.T., Moore, L., Ziegler, A.N., and levison, S. (2015b). Multimarker flow cytometric characterization, isolation and differentiation of neural stem cells and progenitors of the normal and injured mouse subventricular zone. In Neural Surface Antigens: From Basic Biology towards Biomedical Applications, J. Prusac, ed. (Elsevier Press), pp. 175–185.

Buono, K.D., Vadlamuri, D., Gan, Q., and Levison, S.W. (2012). Leukemia inhibitory factor is essential for subventricular zone neural stem cell and progenitor homeostasis as revealed by a novel flow cytometric analysis. Dev. Neurosci. *34*, 449–462.

Carleton, A., Petreanu, L.T., Lansford, R., Alvarez-Buylla, A., and Lledo, P.M. (2003). Becoming a new neuron in the adult olfactory bulb. Nat. Neurosci. *6*, 507–518.

Charalambous, M., Menheniott, T.R., Bennett, W.R., Kelly, S.M., Dell, G., Dandolo, L., and Ward, A. (2004). An enhancer element at the Igf2/H19 locus drives gene expression in both imprinted and non-imprinted tissues. Dev. Biol. *271*, 488–497.

Chen, D.Y., Stern, S.A., Garcia-Osta, A., Saunier-Rebori, B., Pollonini, G., Bambah-Mukku, D., Blitzer, R.D., and Alberini, C.M. (2011). A critical role for IGF-II in memory consolidation and enhancement. Nature *469*, 491–497.

Chen, R.L., Kassem, N.A., Sadeghi, M., and Preston, J.E. (2008). Insulin-like growth factor-ii uptake into choroid plexus and brain of young and old sheep. J. Gerontol. A Biol. Sci. Med. Sci. *63*, 141–148.

Chojnacki, A., Cusulin, C., and Weiss, S. (2012). Adult periventricular neural stem cells: outstanding progress and outstanding issues. Dev. Neurobiol. *72*, 972–989.

Cui, H., Cruz-Correa, M., Giardiello, F.M., Hutcheon, D.F., Kafonek, D.R., Brandenburg, S., Wu, Y., He, X., Powe, N.R., and Feinberg, A.P. (2003). Loss of IGF2 imprinting: a potential marker of colorectal cancer risk. Science *299*, 1753–1755.

DeChiara, T.M., Efstratiadis, A., and Robertson, E.J. (1990). A growth-deficiency phenotype in heterozygous mice carrying an insulin-like growth factor II gene disrupted by targeting. Nature *345*, 78–80.

DeChiara, T.M., Robertson, E.J., and Efstratiadis, A. (1991). Parental imprinting of the mouse insulin-like growth factor II gene. Cell *64*, 849–859.

Farin, H.F., Van Es, J.H., and Clevers, H. (2012). Redundant sources of Wnt regulate intestinal stem cells and promote formation of Paneth cells. Gastroenterology *143*, 1518–1529.e17.

Feil, R., Walter, J., Allen, N.D., and Reik, W. (1994). Developmental control of allelic methylation in the imprinted mouse Igf2 and H19 genes. Development *120*, 2933–2943.

Ferguson-Smith, A.C., Cattanach, B.M., Barton, S.C., Beechey, C.V., and Surani, M.A. (1991). Embryological and molecular investigations of parental imprinting on mouse chromosome 7. Nature *351*, 667–670.

Ferron, S.R., Radford, E.J., Domingo-Muelas, A., Kleine, I., Ramme, A., Gray, D., Sandovici, I., Constancia, M., Ward, A., Menheniott, T.R., et al. (2015). Differential genomic imprinting regulates paracrine and autocrine roles of IGF2 in mouse adult neurogenesis. Nat. Commun. *6*, 8265.

Fevr, T., Robine, S., Louvard, D., and Huelsken, J. (2007). Wnt/beta-catenin is essential for intestinal homeostasis and maintenance of intestinal stem cells. Mol. Cell. Biol. *27*, 7551–7559.

Gao, N., White, P., and Kaestner, K.H. (2009). Establishment of intestinal identity and epithelial-mesenchymal signaling by Cdx2. Dev. Cell *16*, 588–599.

Gelato, M.C., and Vassalotti, J. (1990). Insulin-like growth factor-II: possible local growth factor in pheochromocytoma. J. Clin. Endocrinol. Metab. *71*, 1168–1174.

Giannoukakis, N., Deal, C., Paquette, J., Goodyer, C.G., and Polychronakos, C. (1993). Parental genomic imprinting of the human IGF2 gene. Nat. Genet. *4*, 98–101.

Goodus, M.T., Guzman, A.M., Calderon, F., Jiang, Y., and Levison, S.W. (2015). Neural stem cells in the immature, but not the mature, subventricular zone respond robustly to traumatic brain injury. Dev. Neurosci. *37*, 29–42.

Gregorieff, A., and Clevers, H. (2010). In situ hybridization to identify gut stem cells. Curr. Protoc. Stem Cell Biol. Chapter 2, Unit 2F 1. https://doi.org/10.1002/9780470151808.sc02f01s12.

Gregorieff, A., Pinto, D., Begthel, H., Destree, O., Kielman, M., and Clevers, H. (2005). Expression pattern of Wnt signaling components in the adult intestine. Gastroenterology *129*, 626–638.

Haley, V.L., Barnes, D.J., Sandovici, I., Constancia, M., Graham, C.F., Pezzella, F., Buhnemann, C., Carter, E.J., and Hassan, A.B. (2012). Igf2 pathway dependency of the Trp53 developmental and tumour phenotypes. EMBO Mol. Med. *4*, 705–718.

Harper, J., Burns, J.L., Foulstone, E.J., Pignatelli, M., Zaina, S., and Hassan, A.B. (2006). Soluble IGF2 receptor rescues Apc(Min/+) intestinal adenoma progression induced by Igf2 loss of imprinting. Cancer Res. *66*, 1940–1948.

Ireland, H., Kemp, R., Houghton, C., Howard, L., Clarke, A.R., Sansom, O.J., and Winton, D.J. (2004). Inducible Cre-mediated control of gene expression in the murine gastrointestinal tract: effect of loss of beta-catenin. Gastroenterology *126*, 1236–1246.

Kabiri, Z., Greicius, G., Madan, B., Biechele, S., Zhong, Z., Zaribafzadeh, H., Edison, Aliyev, J., Wu, Y., Bunte, R., et al. (2014). Stroma provides an intestinal stem cell niche in the absence of epithelial Wnts. Development *141*, 2206–2215.

Kato, T., Yokouchi, K., Fukushima, N., Kawagishi, K., Li, Z., and Moriizumi, T. (2001). Continual replacement of newly-generated olfactory neurons in adult rats. Neurosci. Lett. *307*, 17–20.

Keku, T.O., Lund, P.K., Galanko, J., Simmons, J.G., Woosley, J.T., and Sandler, R.S. (2005). Insulin resistance, apoptosis, and colorectal adenoma risk. Cancer Epidemiol. Biomarkers Prev. *14*, 2076–2081.

Kelijman, M. (1991). Age-related alterations of the growth hormone/insulin-like-growth-factor I axis. J. Am. Geriatr. Soc. *39*, 295–307.

Korinek, V., Barker, N., Moerer, P., van Donselaar, E., Huls, G., Peters, P.J., and Clevers, H. (1998). Depletion of epithelial stem-cell compartments in the small intestine of mice lacking Tcf-4. Nat. Genet. *19*, 379–383.

Kuhnert, F., Davis, C.R., Wang, H.T., Chu, P., Lee, M., Yuan, J., Nusse, R., and Kuo, C.J. (2004). Essential requirement for Wnt signaling in proliferation of adult small intestine and colon revealed by adenoviral expression of Dickkopf-1. Proc. Natl. Acad. Sci. U S A *101*, 266–271.

Lamonerie, T., Lavialle, C., Haddada, H., and Brison, O. (1995). IGF-2 autocrine stimulation in tumorigenic clones of a human colon-carcinoma cell line. Int. J. Cancer *61*, 587–592.

Lander, A.D., Kimble, J., Clevers, H., Fuchs, E., Montarras, D., Buckingham, M., Calof, A.L., Trumpp, A., and Oskarsson, T. (2012). What does the concept of the stem cell niche really mean today? BMC Biol. *10*, 19.

Lehtinen, M.K., Zappaterra, M.W., Chen, X., Yang, Y.J., Hill, A.D., Lun, M., Maynard, T., Gonzalez, D., Kim, S., Ye, P., et al. (2011). The cerebrospinal fluid provides a proliferative niche for neural progenitor cells. Neuron *69*, 893–905.

Lim, D.A., and Alvarez-Buylla, A. (2014). Adult neural stem cells stake their ground. Trends Neurosci. *37*, 563–571.

Liu, J.P., Baker, J., Perkins, A.S., Robertson, E.J., and Efstratiadis, A. (1993). Mice carrying null mutations of the genes encoding insulin-like growth factor I (Igf-1) and type 1 IGF receptor (Igf1r). Cell *75*, 59–72.

Lledo, P.M., and Saghatelyan, A. (2005). Integrating new neurons into the adult olfactory bulb: joining the network, life-death decisions, and the effects of sensory experience. Trends Neurosci. *28*, 248–254.

Llorens-Martin, M., and Trejo, J.L. (2011). Multiple birthdating analyses in adult neurogenesis: a line-up of the usual suspects. Front. Neurosci. *5*, 76.

Logan, A., Gonzalez, A.M., Hill, D.J., Berry, M., Gregson, N.A., and Baird, A. (1994a). Coordinated pattern of expression and localization of insulin-like growth factor-II (IGF-II) and IGF-binding protein-2 in the adult rat brain. Endocrinology *135*, 2255–2264.

Logan, A., Oliver, J.J., and Berry, M. (1994b). Growth factors in cns repair and regeneration. ProgGrowthFactorRes *5*, 379–405.

Mellott, T.J., Pender, S.M., Burke, R.M., Langley, E.A., and Blusztajn, J.K. (2014). IGF2 ameliorates amyloidosis, increases cholinergic marker expression and raises BMP9 and neurotrophin levels in the hippocampus of the APPswePS1dE9 Alzheimer's disease model mice. PLoS One *9*, e94287.

Petreanu, L., and Alvarez-Buylla, A. (2002). Maturation and death of adult-born olfactory bulb granule neurons: role of olfaction. J. Neurosci. *22*, 6106–6113.

Pinto, D., Gregorieff, A., Begthel, H., and Clevers, H. (2003). Canonical Wnt signals are essential for homeostasis of the intestinal epithelium. Genes Dev. *17*, 1709–1713.

Porter, E.M., Bevins, C.L., Ghosh, D., and Ganz, T. (2002). The multifaceted Paneth cell. Cell. Mol. Life Sci. *59*, 156–170.

Ramocki, N.M., Wilkins, H.R., Magness, S.T., Simmons, J.G., Scull, B.P., Lee, G.H., McNaughton, K.K., and Lund, P.K. (2008). Insulin receptor substrate-1 deficiency promotes apoptosis in the putative intestinal crypt stem cell region, limits Apcmin/+ tumors, and regulates Sox9. Endocrinology *149*, 261–267.

Ren, H., Yin, P., and Duan, C. (2008). IGFBP-5 regulates muscle cell differentiation by binding to IGF-II and switching on the IGF-II auto-regulation loop. J. Cell Biol. *182*, 979–991.

Romanko, M.J., Rothstein, R.P., and Levison, S.W. (2004). Neural stem cells in the subventricular zone are resilient to hypoxia/ischemia whereas progenitors are vulnerable. J. Cereb. Blood Flow Metab. *24*, 814–825.

Sakatani, T., Kaneda, A., Iacobuzio-Donahue, C.A., Carter, M.G., de Boom Witzel, S., Okano, H., Ko, M.S., Ohlsson, R., Longo, D.L., and Feinberg, A.P. (2005). Loss of imprinting of Igf2 alters intestinal maturation and tumorigenesis in mice. Science *307*, 1976–1978.

Sangiorgi, E., and Capecchi, M.R. (2008). Bmi1 is expressed in vivo in intestinal stem cells. Nat. Genet. *40*, 915–920.

Sato, T., and Clevers, H. (2013). Primary mouse small intestinal epithelial cell cultures. Methods Mol. Biol. *945*, 319–328.

Sato, T., van Es, J.H., Snippert, H.J., Stange, D.E., Vries, R.G., van den Born, M., Barker, N., Shroyer, N.F., van de Wetering, M., and Clevers, H. (2011). Paneth cells constitute the niche for Lgr5 stem cells in intestinal crypts. Nature *469*, 415–418.

Sato, T., Vries, R.G., Snippert, H.J., van de Wetering, M., Barker, N., Stange, D.E., van Es, J.H., Abo, A., Kujala, P., Peters, P.J., et al. (2009). Single Lgr5 stem cells build crypt-villus structures in vitro without a mesenchymal niche. Nature *459*, 262–265.

Shinar, D.M., Endo, N., Halperin, D., Rodan, G.A., and Weinreb, M. (1993). Differential expression of insulin-like growth factor-I (IGF-I) and IGF-II messenger ribonucleic acid in growing rat bone. Endocrinology *132*, 1158–1167.

Silver, D.P., and Livingston, D.M. (2001). Self-excising retroviral vectors encoding the Cre recombinase overcome Cre-mediated cellular toxicity. Mol. Cell *8*, 233–243.

Stylianopoulou, F., Herbert, J., Soares, M.B., and Efstratiadis, A. (1988). Expression of the insulin-like growth factor II gene in the choroid plexus and the leptomeninges of the adult rat central nervous system. Proc. Natl. Acad. Sci. U S A *85*, 141–145.

Takeda, N., Jain, R., LeBoeuf, M.R., Wang, Q., Lu, M.M., and Epstein, J.A. (2011). Interconversion between intestinal stem cell populations in distinct niches. Science *334*, 1420–1424.

Tetteh, P.W., Farin, H.F., and Clevers, H. (2014). Plasticity within stem cell hierarchies in mammalian epithelia. Trends Cell Biol. *25*, 100–108.

Tuttle, A.H., Rankin, M.M., Teta, M., Sartori, D.J., Stein, G.M., Kim, G.J., Virgilio, C., Granger, A., Zhou, D., Long, S.H., et al. (2010). Immunofluorescent detection of two thymidine analogues (CldU and IdU) in primary tissue. J. Vis. Exp., 2166. https://doi.org/10.3791/2166.

van der Flier, L.G., and Clevers, H. (2009). Stem cells, self-renewal, and differentiation in the intestinal epithelium. Annu. Rev. Physiol. *71*, 241–260.

van Es, J.H., Haegebarth, A., Kujala, P., Itzkovitz, S., Koo, B.K., Boj, S.F., Korving, J., van den Born, M., van Oudenaarden, A., Robine, S., et al. (2012). A critical role for the Wnt effector Tcf4 in adult intestinal homeostatic self-renewal. Mol. Cell. Biol. *32*, 1918–1927.

Vega, C.J., and Peterson, D.A. (2005). Stem cell proliferative history in tissue revealed by temporal halogenated thymidine analog discrimination. Nat. Methods *2*, 167–169.

Winner, B., Cooper-Kuhn, C.M., Aigner, R., Winkler, J., and Kuhn, H.G. (2002). Long-term survival and cell death of newly generated neurons in the adult rat olfactory bulb. Eur. J. Neurosci. *16*, 1681–1689.

Yang, M., and Crawley, J.N. (2009). Simple behavioral assessment of mouse olfaction. Curr. Protoc. Neurosci. Chapter 8:Unit 8.24. https://doi.org/10.1002/0471142301.ns0824s48.

Yang, Z., You, Y., and Levison, S.W. (2008). Neonatal hypoxic/ischemic brain injury induces production of calretinin-expressing interneurons in the striatum. J. Comp. Neurol. *511*, 19–33.

Yee, D., Cullen, K.J., Paik, S., Perdue, J.F., Hampton, B., Schwartz, A., Lippman, M.E., and Rosen, N. (1988). Insulin-like growth factor II mRNA expression in human breast cancer. Cancer Res. *48*, 6691–6696.

Yin, X., Farin, H.F., van Es, J.H., Clevers, H., Langer, R., and Karp, J.M. (2014). Niche-independent high-purity cultures of Lgr5+ intestinal stem cells and their progeny. Nat. Methods *11*, 106–112.

Yu, S., Tong, K., Zhao, Y., Balasubramanian, I., Yap, G.S., Ferraris, R.P., Bonder, E.M., Verzi, M.P., and Gao, N. (2018). Paneth cell multipotency induced by notch activation following injury. Cell Stem Cell *23*, 46–59.e45.

Zhao, C., Deng, W., and Gage, F.H. (2008). Mechanisms and functional implications of adult neurogenesis. Cell *132*, 645–660.

Ziegler, A.N., Chidambaram, S., Forbes, B.E., Wood, T.L., and Levison, S.W. (2014). Insulin-like growth factor-II (IGF-II) and IGF-II analogs with enhanced insulin receptor-a binding affinity promote neural stem cell expansion. J. Biol. Chem. *289*, 4626–4633.

Ziegler, A.N., Schneider, J.S., Qin, M., Tyler, W.A., Pintar, J.E., Fraidenraich, D., Wood, T.L., and Levison, S.W. (2012). IGF-II promotes stemness of neural restricted precursors. Stem Cells *30*, 1265–1276.

Stem Cell Reports, Volume *12*

Supplemental Information

Insulin-like Growth Factor II: An Essential Adult Stem Cell Niche Constituent in Brain and Intestine

Amber N. Ziegler, Qiang Feng, Shravanthi Chidambaram, Jaimie M. Testai, Ekta Kumari, Deborah E. Rothbard, Miguel Constancia, Ionel Sandovici, Tara Cominski, Kevin Pang, Nan Gao, Teresa L. Wood, and Steven W. Levison

Supplemental Figures

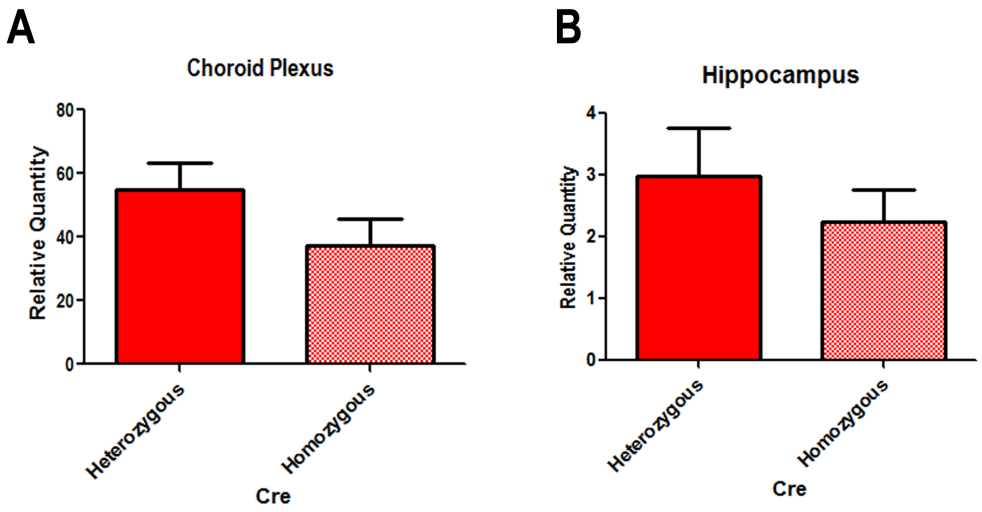

Figure S1. Comparison of *Igf2* RNA in mice heterozygous and homozygous for Cre. Related to Figure 1. Choroid plexus (**A**) and hippocampus (**B**) *Igf2* expression was compared after recombination induced by tamoxifen administration to mice heterozygous or homozygous for Cre and homozygous for floxed *Igf2*. No significant difference was found. n=5 WT and n=12 iKO mice. Error bars represent SEM.

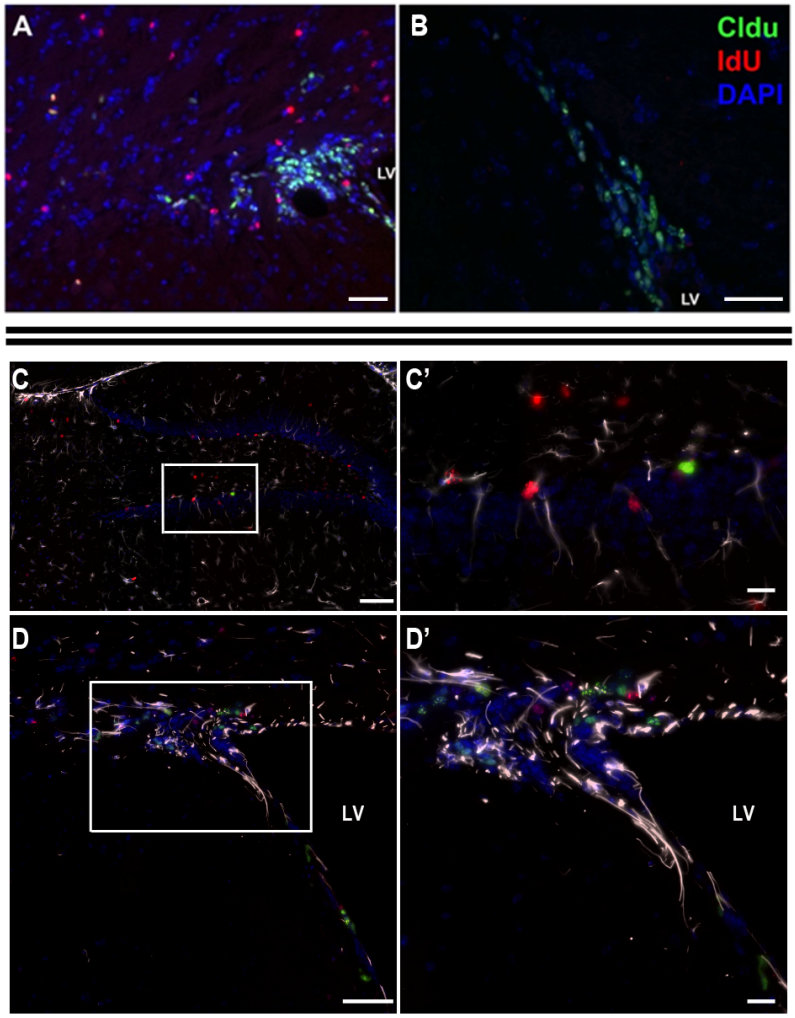

Figure S2. Dual nucleotide staining validity test. Related to Figures 2 and 3.
IdU antibodies have been reported to cross-react and recognize CldU analog, therefore, studies were performed to establish that the IdU antibody that we used did not cross react with CldU. Tissue from a mouse that received IdU and CldU analogs (**A**) was stained for CldU (green) and IdU (red) GFAP (white) panels (**C, D**) and counterstained with DAPI (blue). (**B**), Tissue from a mouse that received only the CldU analog was stained similarly. In our hands there was no cross-reactivity between IdU antibody and CldU analog (**A, B**). IdU was administered for 3 weeks followed by a 2-week washout, and then a single injection of CldU was given 4 hours prior to tissue collection (**C, D**). Very few CldU cells (green) were detected in the hippocampus (**C**) and inset (**C'**). By contrast, the SVZ contained many CldU positive (green) cells (**D**) and inset (**D'**). Double positive cells (yellow) were not detected in hippocampus or SVZ. LV = lateral ventricle. Scale bars = 100 µM (A, B, C, and D) and 20 µM (C' and D').

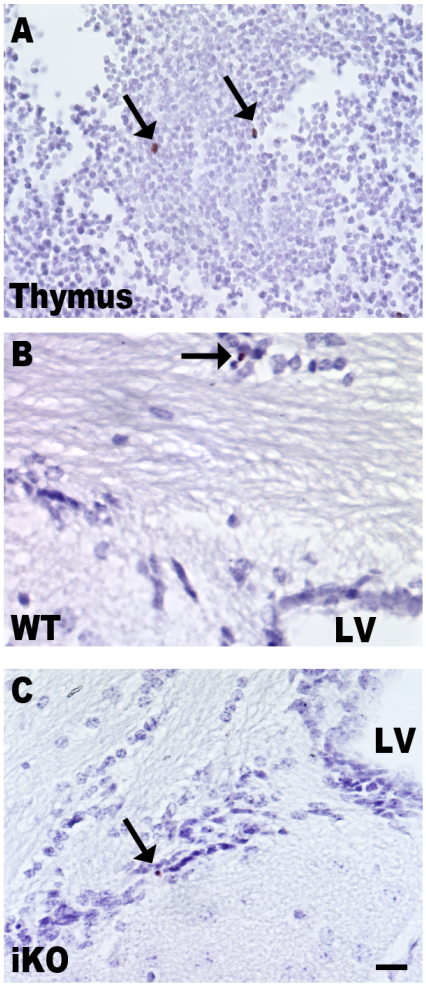

Figure S3. *In-situ* end labeling reveals no increase in cell death within the SVZ or the SGZ. Related to Figures 2, 3 and Table 1.

In-situ end labeling (ISEL) was performed on mouse thymus (A) (positive control tissue) and on WT (**B**) and iKO (**C**) mouse forebrains; lateral ventricle (LV). $ISEL^{+}$ cells, which have condensed reddish-brown nuclei, were rare in the SVZ and no positive cells were observed in the hippocampus. Sections were counterstained with hematoxylin. Scale bar = 50 μM.

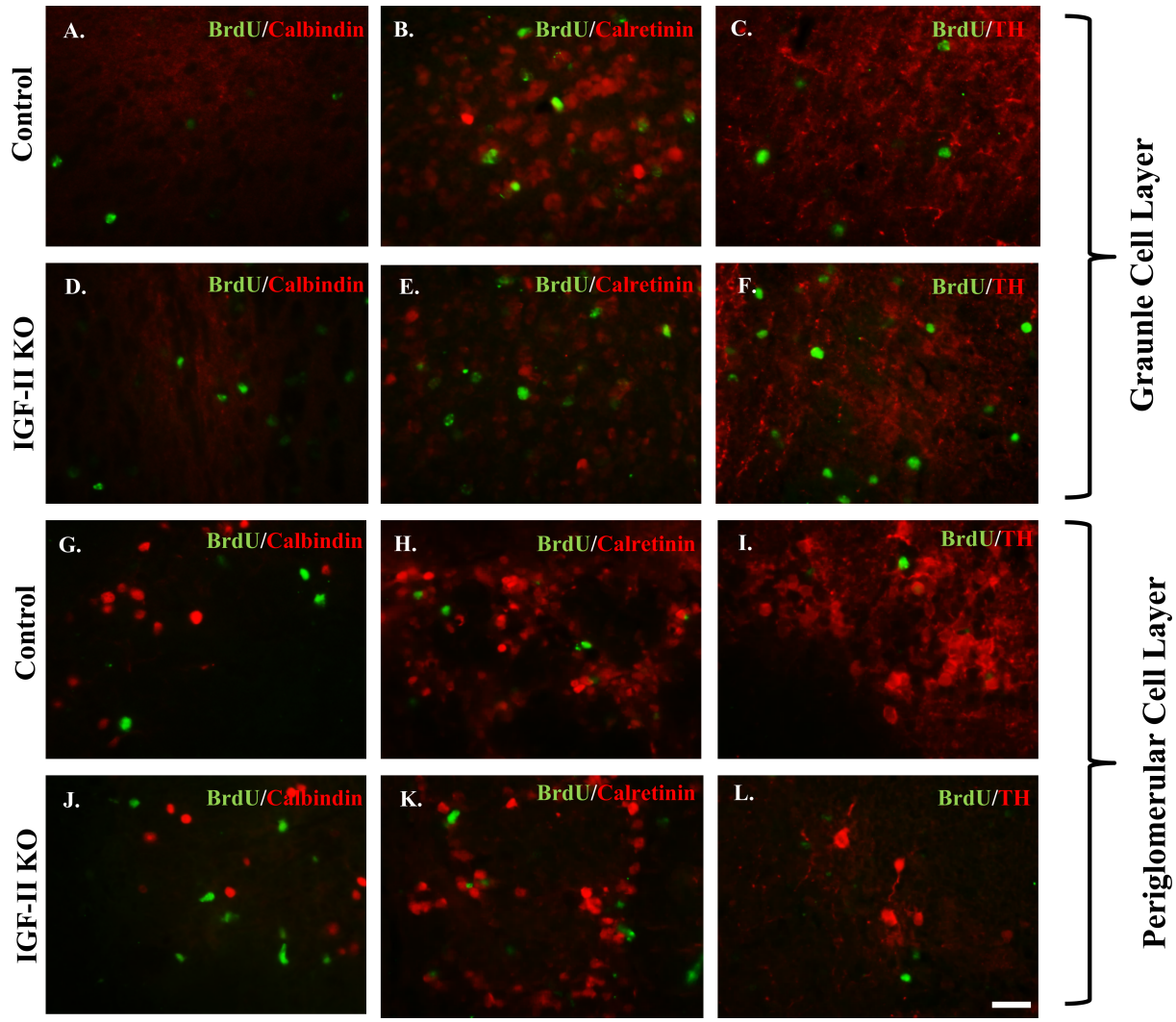

Figure S4: Representative images of BrdU and calbindin, calretinin and tyrosine hydroxylase immunofluorescence in the olfactory bulbs of WT and iKO mice. Related to Figure 3.
WT (**A-C, G-I**) and iKO (**D-F, J-L**) olfactory bulb granule cell layer (**A-F**) and periglomerular layer (**G-L**) stained for BrdU, calbindin (**A, D, G, J**), calretinin (**B, E, H, K**) and tyrosine hydroxylase (**C, F, I, L**), 5 weeks after BrdU administration. Scale bar = 100 μm.

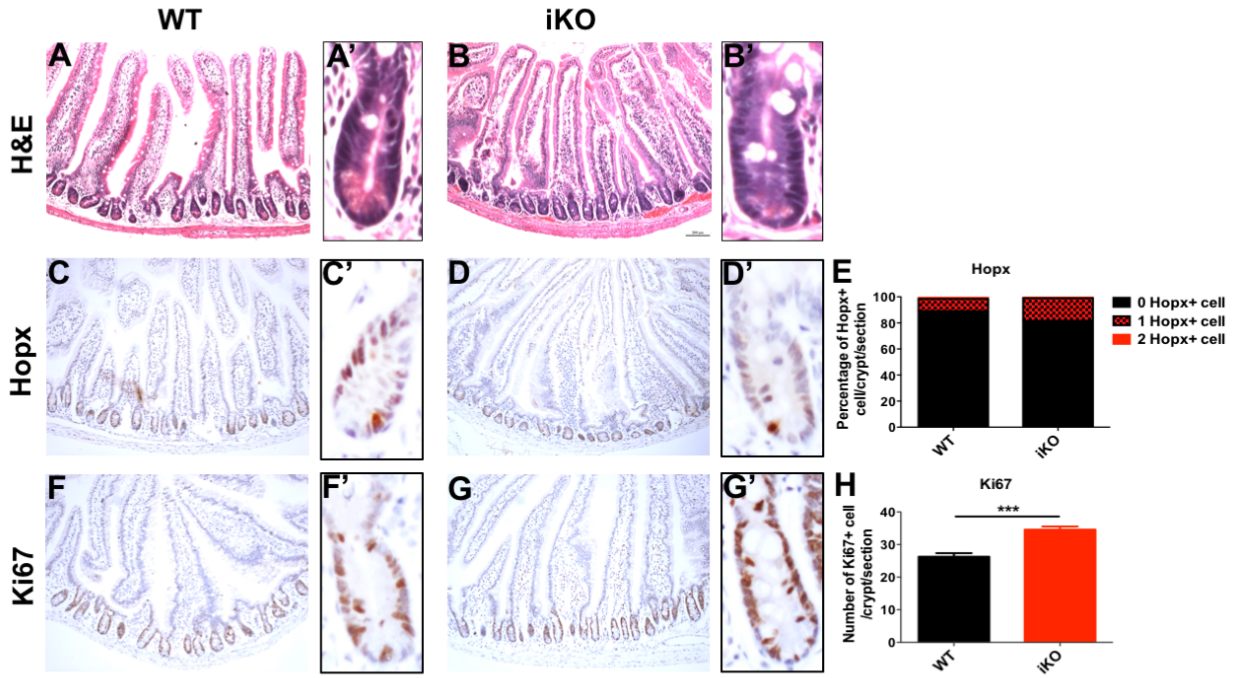

Figure S5: Long-term deletion of *Igf2* showed a compensatory phenotype in small intestine. Related to Figure 5.

Igf2 deletion was induced using 5 doses of tamoxifen administered every 3 days. Small intestine of WT and iKO mice were stained for H&E (**A, A', B, B'**), Hopx (**C, C', D, D', E**; for the quiescent stem cell), Ki67 (**F, F', G, G', H**; for proliferative progenitor cell) and Lysozyme (**I, I', J, J', K**; for Paneth cell) n=3 (WT) and 3 (iKO) mice. Scale bar = 200 μm. *, $p<0.05$; ***, $p<0.001$ by Student's T test. Error bars represent SEM.

Supplemental Experimental Procedures - Behavioral Tests

Buried Food test: A simple test for mouse olfaction was followed as described by Yang and Crawley (2009. Briefly mice were fasted for 12 hours and then placed into a clean test chamber where a piece of cereal was buried under the bedding. The mice were pre-exposed to the test chamber and the cereal prior to the test. All mice consumed the cereal prior to the test. The latency (seconds) to find the hidden cereal was recorded.

Morris Water Maze:
Hidden Platform: The water maze consisted of a pool with a 0.97 meter diameter and a platform (10 cm in diameter) placed in the target quadrant (TQ) submerged under water made opaque with white non-toxic paint (Art Minds Tempera Paint, Michael's Inc). Several visual cues were dispersed throughout the room. Mice were tested in the Morris Water Maze for 5 consecutive days. Day 1 consisted of 1 pre-training session. On days 2-5, mice received 2 training sessions per day, one in the morning and one in the afternoon. The latency to find the platform was measured for each trial. Each training session consisted of 4 trials with the mouse started in a different quadrant of the maze each time, omitting placement in the TQ. On day 6, mice received a probe trial where the platform was removed and the time spent searching the TQ was measured.

Visible Platform: Mice were placed in the maze containing a visible platform by extending a patterned cylinder beyond the surface of the water. Mice were given 60 seconds to swim to the platform. Each mouse received 3 sessions with 1 hour between each session of 4 trials each; each trial lasted 60 seconds or the time it took the mouse to reach to the platform. Mice were subjected to the visible platform task on day 7 of the experiment to ensure that visual and motor abilities were normal.

Open Field: Horizontal locomotor activity was measured using the open field photobeam activity system (PAS; SD Instruments). PAS recording software was programmed to collect data over 6 phases consisting of a 5 min interval per phase. The animals were placed in the center of the open field. Photobeam breaks were converted to total distance traveled in cm using the PAS reporter software (version 2). The resting time parameter in the software was set at 4 seconds. A center area was defined using the PAS software as an 8 by 8 inches square in the center of the arena from which Photobeam breaks were also assessed.